Transient elastography with controlled attenuation parameter versus two-dimensional shear wave elastography with attenuation imaging for the evaluation of hepatic steatosis and fibrosis in NAFLD

Jung Wook Seo[1]*, Youe Ree Kim[2]*, Jong Keon Jang[3], So Yeon Kim[3], Young Youn Cho[4], Eun Sun Lee[5], Dong Ho Lee[6]

[1]Department of Radiology, Ilsan Paik Hospital, Inje University College of Medicine, Goyang; [2]Department of Radiology, Wonkwang University Hospital, Wonkwang University College of Medicine, Iksan; [3]Department of Radiology and Research Institute of Radiology, Asan Medical Center, University of Ulsan College of Medicine, Seoul; [4]Department of Internal Medicine, [5]Department of Radiology, Chung-Ang University Hospital, Seoul; [6]Department of Radiology, Seoul National University Hospital, Seoul, Korea

Purpose: This study compared the controlled attenuation parameter (CAP) to attenuation imaging (ATI) in the diagnosis of steatosis and transient elastography (TE) to two-dimensional shear wave elastography (2D-SWE) for the diagnosis of fibrosis in a prospectively constructed nonalcoholic fatty liver disease (NAFLD) patient cohort.

Methods: Participants who underwent TE with CAP were included from a previously constructed NAFLD cohort with multiparametric ultrasound data. The degree of hepatic steatosis and stage of liver fibrosis were assessed. Diagnostic performance was evaluated using the area under the receiver operating characteristic curve (AUROC) for the grades of steatosis (S1–3) and fibrosis (F0–F4).

Results: There were 105 participants. The distribution of hepatic steatosis grades (S0–S3) and liver fibrosis stages (F0–F4) was as follows: S0, n=34; S1, n=41; S2, n=22; S3, n=8; F0, n=63; F1, n=25; F2, n=5; F3, n=7; and F4, n=5. No significant difference was found between CAP and ATI in detecting ≥S1 (AUROC: 0.93 vs. 0.93, P=0.956) or ≥S2 (0.94 vs. 0.94, P=0.769). However, the AUROC of ATI in detecting ≥S3 was significantly higher than that of CAP (0.94 vs. 0.87, P=0.047). Regarding the detection of liver fibrosis, no significant difference was found between TE and 2D-SWE. The AUROCs of TE and 2D-SWE were as follows: ≥F1, 0.94 vs. 0.89 (P=0.107); ≥F2, 0.89 vs. 0.90 (P=0.644); ≥F3, 0.91 vs. 0.90 (P=0.703); and ≥F4, 0.88 vs. 0.92 (P=0.209).

Conclusion: 2D-SWE and TE showed comparable diagnostic performance in assessing liver fibrosis, and ATI provided significantly better performance in detecting ≥S3 steatosis than CAP.

Keywords: Liver cirrhosis; Fatty liver; Elasticity imaging techniques

Key points: Two-dimensional shear wave elastography (2D-SWE) provided comparable diagnostic performance in assessing the stage of liver fibrosis to that of transient elastography (TE). Attenuation imaging (ATI) provided significantly better diagnostic accuracy in detecting severe steatosis (≥S3) than the controlled attenuation parameter from TE. A multiparametric approach using 2D-SWE with ATI might be helpful and could be used as a primary imaging test for the evaluation of nonalcoholic fatty liver disease patients.

ULTRASONOGRAPHY

ORIGINAL ARTICLE

https://doi.org/10.14366/usg.22212
eISSN: 2288-5943
Ultrasonography. 2023 Mar 10. Epub ahead of print

Received: December 20, 2022
Revised: February 23, 2023
Accepted: March 10, 2023

Correspondence to:
Dong Ho Lee, MD, Department of Radiology, Seoul National University Hospital, 101 Daehak-ro, Jongno-gu, Seoul 03080, Korea

Tel. +82-2-2072–0348
Fax. +82-2-743-6385
E-mail: dhlee.rad@gmail.com

*These authors contributed equally to this work.

How to cite this article:
Seo JW, Kim YR, Jang JK, Kim SY, Cho YY, Lee ES, et al. Transient elastography with controlled attenuation parameter versus two-dimensional shear wave elastography with attenuation imaging for the evaluation of hepatic steatosis and fibrosis in NAFLD. Ultrasonography 2023 Mar 10 [Epub]. https://doi.org/10.14366/usg.22212

Introduction

Globally, one-quarter of adults have nonalcoholic fatty liver disease (NAFLD), and this number is expected to increase by 18% by 2030 and by about 50% by 2040 [1–5]. NAFLD is a common disease and its importance can be overlooked; however, it can be accompanied by other comorbid conditions, including obesity, dyslipidemia, type 2 diabetes, and metabolic syndrome [6,7]. Moreover, NAFLD comprises a group of diseases with various prognoses that can develop from simple hepatic steatosis, such as uncomplicated NAFLD, nonalcoholic steatohepatitis (NASH) accompanied by hepatocyte ballooning and necroinflammation, liver cirrhosis, and eventually hepatocellular carcinoma [6,8,9]. NASH develops in approximately 20% of NAFLD patients, of whom roughly 20% progress to cirrhosis [1,10]. Cirrhosis due to NAFLD is already a leading cause of transplantation in women in North America [11]. Therefore, timely detection and proper management of NAFLD are important.

Liver biopsy is the gold standard for diagnosing fatty changes in the liver and accompanying fibrosis despite its innate disadvantages, such as invasiveness and bleeding risk [12]. However, since it is difficult to perform a biopsy in all patients with suspected NAFLD, blood chemistry and various imaging tests have been used and studied for the management of NAFLD [13,14]. Transient elastography (TE) with the controlled attenuation parameter (CAP) has been developed and introduced into clinical practice. Liver stiffness (LS) measurements using TE have shown good diagnostic performance for staging liver fibrosis and detecting cirrhosis [6]. Regarding hepatic steatosis, studies on the quantitative evaluation of hepatic steatosis using CAP, which can quantify the degree of ultrasound (US) beam attenuation by the tissue, have also been conducted for several years and have provided promising results [15–19]. In addition to TE, two-dimensional shear wave elastography (2D-SWE) has emerged as another noninvasive method to evaluate liver fibrosis, for which studies have reported a good diagnostic performance, even better than TE [20–23]. Real-time B-mode US-based attenuation imaging (ATI) has recently been introduced and reported to have high diagnostic performance in detecting hepatic steatosis by calculating the degree of US beam attenuation, similar to the CAP from TE [24–28]. Relative to TE with CAP, 2D-SWE with ATI has several theoretical merits, including easy incorporation into routine B-mode US examinations and accurate selection of the measurement region of interest (ROI) guided by simultaneously provided B-mode images, which could lead to more accurate and reliable measurements. However, whether these theoretical advantages of 2D-SWE with ATI could improve the diagnostic performance in assessing liver fibrosis and hepatic steatosis compared to TE with CAP has not been evaluated. Therefore, the purpose of this study was to compare CAP with ATI in the diagnosis of steatosis and to compare TE with 2D-SWE in the diagnosis of fibrosis in a NAFLD patient cohort.

Materials and Methods

Compliance with Ethical Standards

The institutional review board (IRB) of each participating center approved this retrospective analysis of the previous cohort (IRB number: H-2210-139-1373 for Seoul National University Hospital, WKUH 2022-11-012 for Wonkwang University Hospital, ISPAIK 2022-10-006 for Ilsan Paik Hospital, 2210-005-19439 for Chung-Ang University Hospital, 2022-1584 for Asan Medical Center), and the requirement for written informed consent was waived by the IRB because of this study's retrospective design.

Study Design

This study was a retrospective analysis of a previous NAFLD cohort constructed from a multicenter study conducted to confirm the diagnostic ability of a multiparametric US approach for patients with NAFLD (study identifier: KCT0004326) [29]. In the previous multicenter study, patients with elevation of liver enzyme or clinical suspicion of NASH were enrolled using the following criteria: (1) no history of positivity for hepatitis B virus surface antigen, anti-hepatitis C virus, hepatitis C virus RNA, and hepatitis B virus DNA; (2) no history of excessive alcohol consumption greater than the recommended limit (>14 UK units/wk for women and >21 UK units/wk for men; 1 UK unit=10 mL of pure alcohol) [29]. Patients having liver pathology other than NAFLD on histopathologic examinations were also excluded from the analysis. In the previous multicenter study, potential living liver donors who underwent liver biopsy to evaluate NAFLD for a decision regarding liver donor eligibility were also enrolled. Among the 132 participants of the previous study, participants who met the following inclusion criteria were enrolled in this study: (1) available results of TE with CAP and (2) reliable LS measurement results obtained from TE.

2D-SWE and ATI

As a prospectively designed study, five abdominal radiologists from five institutions had two meetings on 2D-SWE and ATI measurement protocols to establish a unified measurement method. The unified measurement protocols for 2D-SWE and ATI were maintained among the five institutions during the study period. All US examinations were performed at each institution using US scanners (Aplio i800, Canon Medical Systems, Otawara, Japan) with a 1–8-MHz convex probe (PVI-475BX). All participants were instructed to fast for at least 6 h before the US examination. The US

examination was performed in a supine position with the right arm extended above the head to obtain an optimal window through intercostal space stretching. The measurement ROIs of 2D-SWE and ATI were set as close as possible to the planned area of the liver biopsy, which was performed in the right anterior section, where the intercostal approach was possible. To avoid reverberation artifacts of the liver capsule, the sample box was placed at least 1 cm below the liver capsule according to liver elasticity imaging guidelines [30,31]. After each participant was asked to hold their breath in an intermediate state, a sample box of 2D-SWE measuring 1.5×1.5 cm was placed on the grayscale image of the liver parenchyma. Then, a 1-cm circular measurement ROI was placed within a sample box to obtain the LS value. LS values were measured 10 times, and the median value was used for further analysis. The 2D-SWE measurements were considered reliable if the interquartile range (IQR)/median value was less than 30%, according to the liver elastography guidelines originally developed for TE [30,31]. After 2D-SWE evaluation, ATI was performed in the right hepatic lobe through the intercostal window. A large sample box was placed on the entire right hepatic lobe parenchyma, and a 2×4-cm square measurement ROI was placed in the sample box, avoiding areas of reverberation artifacts or large hepatic vessels. The attenuation coefficient (AC) in units of dB/cm/MHz appeared immediately after the placement of the measurement ROI at the bottom of the image. At the bottom of the image, the AC appears together with the reliable measurement coefficient (R-value), and an R-value of 0.80 or higher was considered to indicate a reliable measurement. The AC was measured five times, and the median value was used.

TE and CAP Measurements

FibroScan (Echosens, Paris, France) was performed on the same day as the 2D-SWE test and a biopsy was performed. FibroScan examinations were performed by a radiologic technician at each center who was blinded to the patient's clinical information and the results of 2D-SWE with ATI. The equipment used was a FibroScan 502 touch model, and each center was equipped with both an M probe (n=74) and an XL probe (n=31). Patients were placed in the supine position with their right arm fully abducted, and measurements were performed in the right hepatic lobe through the intercostal space. FibroScan devices use vibration-controlled TE technology to simultaneously measure LS and CAP. The CAP was designed to measure liver US attenuation at 3.5 MHz on both M and XL probes on signals acquired by FibroScan. CAPs were calculated only if the associated LS measurement was valid and the same signal was used to measure liver stiffness. CAP and LS measurements were expressed as dB/m and kPa, respectively. LS measurements were considered reliable if the IQR/median value was less than 30%, according to the liver elastography guidelines originally developed for TE [30,31]. Only tests with at least 10 valid individual measurements were considered valid.

Liver Biopsy and Histopathologic Evaluation

A biopsy was performed in the right anterior section of the liver through the intercostal plane. Using an 18-gauge biopsy gun, liver specimens approximately 2 cm in length were collected two or three times from the patient. The liver tissue obtained was fixed in formalin solution, and hematoxylin/eosin and Masson trichrome staining were performed to evaluate the pathology and fibrosis of NAFLD. The pathological evaluation of liver tissue was performed at each center by a pathologist (i.e., five pathologists with more than 5 years of experience in liver pathology at five centers) who was blinded to the patient's clinical information. The degree of hepatic steatosis, lobular inflammatory activity, hepatocyte ballooning, and stage of liver fibrosis were evaluated using the NASH–clinical research network scoring system, and each center used the same criteria for histopathologic examinations [32]. Steatosis was graded from 0 to 3 (S0–S3), hepatocyte ballooning from 0 to 2 (B0–B2), lobular inflammatory activity from 0 to 3 (I0–I3), and fibrosis stage from 0 to 4 (F0–F4). For the evaluation of hepatic steatosis, the following criteria were used: S0, when the area of steatosis on low to medium power evaluation was <5%; S1, 5%–33%; S2, >33%–66%; and S3, >66%.

Statistical Analysis

Continuous variables are expressed as medians with IQRs, and categorical variables as percentages. For the univariate analysis, continuous variables were compared using the Mann-Whitney U test and categorical variables were compared using the Fisher exact test. Univariate and multivariate linear regression analyses were used to determine the significant determinant factors for AC from ATI, LS values from 2D-SWE, CAP from TE, and LS values from TE, and all variables with a P-value less than 0.05 in the univariate analysis were included in the multivariate analysis. Receiver operating characteristic (ROC) curve analysis was performed to evaluate the diagnostic performance for detecting each grade of hepatic steatosis and each stage of liver fibrosis, and the area under the ROC curve (AUROC) was calculated with 95% confidence intervals. To compare AUROCs between two modalities, the DeLong method was used. Cutoff values were determined to maximize the Youden index. The sensitivity, specificity, positive predictive value (PPV), and negative predictive value (NPV) were calculated for each cutoff value. All statistical analyses were conducted using SPSS version 28 (IBM Corp., Armonk, NY, USA) and MedCalc software package version 15.2 (MedCalc, Mariakerke, Belgium).

Results

Patient Characteristics

This study was a retrospective analysis of data from a previous multicenter study evaluating the usefulness of multiparametric US in NAFLD patients (identifier: KCT0004326). In the previous multicenter study, 132 participants were analyzed. Among them, 27 participants were excluded from this study due to the absence of an available TE examination (n=24) or unreliable measurement results of TE (n=3). The remaining 105 participants were included in the final study (Fig. 1). Among them, 58 participants were potential living liver donors, and detailed information regarding the enrollment process is given in the Supplementary Material 1. The baseline characteristics of the participants are summarized in Table 1.

Evaluation of Hepatic Steatosis Using CAP and Attenuation Coefficient

The factors affecting CAP from TE and AC from ATI are summarized in Supplementary Table 1. In multivariate analysis, the grade of hepatic steatosis on histopathology (P<0.01) was the only significant factor affecting AC from ATI. Regarding CAP from TE, the degree of hepatic steatosis (P<0.01), patients' age (P=0.016), and body mass index (BMI) (P=0.005) were significantly associated with CAP values in the multivariate analysis.

The distribution of hepatic steatosis grades was as follows: S0, n=34 (32.4%); S1, n=41 (39.0%); S2, n=22 (21.0%); and S3, n=8 (7.6%). The baseline characteristics of the patients according to the grade of hepatic steatosis are summarized in Supplementary Table 2. The diagnostic performance, including the AUROC and cutoff value with the corresponding sensitivity, specificity, PPV, and NPV, for detecting each grade of hepatic steatosis determined by ROC analysis, are presented in Table 2 and Fig. 2. CAP values from TE and AC from ATI increased with the progression of hepatic steatosis grades. The median value of CAP from TE was 196 dB/m (IQR, 168 to 225 dB/m) in S0; 262 dB/m (IQR, 230 to 287 dB/m) in S1; 322 dB/m (IQR, 309 to 349 dB/m) in S2; and 339 dB/m (IQR, 312 to 363 dB/m) in S3 (P<0.001). The median value of AC from ATI was 0.55 dB/cm/MHz (IQR, 0.51 to 0.59 dB/cm/MHz) in S0; 0.67 dB/cm/MHz (IQR, 0.61 to 0.73 dB/cm/MHz) in S1; 0.80 dB/cm/MHz (0.74 to 0.87 dB/cm/MHz) in S2; and 0.91 dB/cm/MHz (IQR, 0.85 to 0.98 dB/cm/MHz) in S3 (P<0.001).

The AUROC of CAP from TE was 0.93 for detecting ≥S1, 0.94 for detecting ≥S2, and 0.87 for detecting ≥S3. AUROC of AC from ATI was 0.93 for detecting ≥S1, 0.94 for detecting ≥S2, and 0.94 for detecting ≥S3. There was no significant difference in the detection of ≥S1 and ≥S2 between CAP from TE and AC. However, the AUROC of AC from ATI for detecting ≥S3 was significantly higher than that of CAP from TE (0.94 vs. 0.87, P=0.047). Regarding the sensitivity of detecting ≥S3, both CAP and AC yielded 100% sensitivity. However, the specificity of AC for detecting ≥S3 was 85% (82/97), which was significantly higher than that of CAP (72%, 70/97; P=0.036). The diagnostic performance of CAP and AC from ATI in detecting each grade of hepatic steatosis was also assessed according to patients' BMI (i.e., BMI <25 kg/m^2 vs. BMI ≥25 kg/m^2), and the results are given in Supplementary Tables 3 and 4.

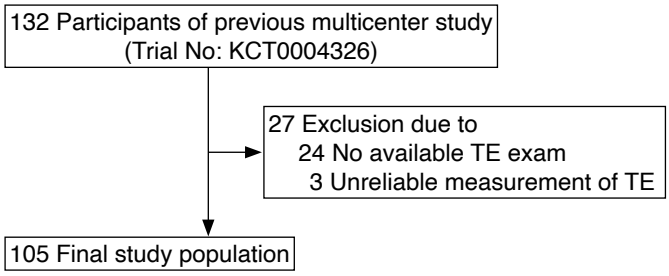

Fig. 1. Flow diagram showing patient selection details. TE, transient elastography.

Table 1. Patient characteristics

Parameter	Value
Age (year)	36.0 (27.0–49.5)
Sex (male:female)	53:52
Body mass index (kg/m^2)	24.2 (22.1–27.2)
Hypertension	31 (29.5)
Diabetes mellitus	20 (19.0)
ALT (IU/L)	21.0 (12.0–50.0)
AST (IU/L)	22.0 (17.0–44.5)
Albumin (mg/dL)	4.3 (4.1–4.5)
Total bilirubin (mg/dL)	0.6 (0.4–0.9)
PT-INR	1.01 (0.98–1.08)
Fibrosis stage	
F0	63 (60.0)
F1	25 (23.8)
F2	5 (4.8)
F3	7 (6.6)
F4	5 (4.8)
Steatosis grade	
S0	34 (32.4)
S1	41 (39.0)
S2	22 (21.0)
S3	8 (7.6)

Values are presented as median (IQR) or number (%).
ALT, alanine aminotransferase; AST, aspartate aminotransferase; PT-INR, prothrombin time–international normalized ratio; IQR, interquartile range.

Table 2. Evaluation of steatosis using the attenuation coefficient and controlled attenuation parameter

	≥S1 (≥5% steatosis)	≥S2 (≥34% steatosis)	≥S3 (≥67% steatosis)
Attenuation coefficient from ATI			
AUROC (95% CI)	0.93 (0.86–0.97)	0.94 (0.88–0.98)	0.94 (0.88–0.98)
Prevalence (n)	71	30	8
Cutoff (dB/cm/MHz)	0.62	0.70	0.78
Sensitivity	0.83 (59/71)	0.93 (28/30)	1.00 (8/8)
Specificity	0.97 (33/34)	0.84 (63/75)	0.85 (82/97)
PPV	0.98 (59/60)	0.70 (28/40)	0.35 (8/23)
NPV	0.73 (33/45)	0.97 (63/65)	1.00 (82/82)
Controlled attenuation parameter from TE			
AUROC (95% CI)	0.93 (0.86–0.97)	0.94 (0.87–0.98)	0.87 (0.79–0.93)
Prevalence (n)	71	30	8
Cutoff (dB/m)	240	285	298
Sensitivity	0.82 (58/71)	0.93 (28/30)	1.00 (8/8)
Specificity	0.94 (32/34)	0.87 (65/75)	0.72 (70/97)
PPV	0.97 (58/60)	0.74 (28/38)	0.23 (8/35)
NPV	0.71 (32/45)	0.97 (65/67)	1.00 (70/70)

ATI, attenuation imaging; AUROC, area under the receiver operating characteristic curve; CI, confidence interval; PPV, positive predictive value; NPV, negative predictive value; TE, transient elastography.

Evaluation of Liver Fibrosis Using LS from TE and 2D-SWE

The significant determinant factors for LS values from TE and 2D-SWE are summarized in Supplementary Table 1. Regarding LS from TE, the stage of liver fibrosis (P<0.01) and grade of hepatocyte ballooning (P=0.01) were identified as significant factors in the multivariate analysis. The stage of liver fibrosis (P=0.01) and BMI (P=0.007) were significantly associated with LS based on 2D-SWE in the multivariate analysis.

The distribution of liver fibrosis stages on histopathology was as follows: F0, n=63 (60.0%); F1, n=25 (23.8%); F2, n=5 (4.8%); F3, n=7 (6.6%); and F4, 5 (4.8%). The baseline characteristics of the patients according to the stage of liver fibrosis are summarized in Supplementary Table 5. The diagnostic performance, including the AUROC and cutoff value with corresponding sensitivity, specificity, PPV, and NPV, for detecting each stage of liver fibrosis determined by ROC analysis is given in Table 3 and Fig. 3. Both LS values from TE and 2D-SWE increased with the progression of the liver fibrosis stage. The AUROC of LS from TE was 0.94 for detecting ≥F1, 0.89 for detecting ≥F2, 0.91 for detecting ≥F3, and 0.92 for detecting ≥F4. The AUROC of LS from 2D-SWE was 0.89 for detecting ≥F1, 0.90 for detecting ≥F2, 0.90 for detecting ≥F3, and 0.88 for detecting ≥F4. There was no significant difference between LS from TE and LS from 2D-SWE in the detection of any stage of liver fibrosis. The diagnostic performance of TE and 2D-SWE in detecting each stage of liver fibrosis was also assessed according to patients' BMI (i.e., BMI <25 kg/m^2 vs. BMI ≥25 kg/m^2), and the results are given in Supplementary Tables 6 and 7.

Discussion

The present study aimed to conduct a head-to-head comparison in order to determine whether there was a diagnostic difference between 2D-SWE with ATI and TE with CAP in the evaluation of NAFLD patients using the histopathologic examination as the reference standard. This study showed comparable results in diagnosing fibrosis, and there was no significant difference between S1 and S2 in diagnosing steatosis, but ATI showed useful results in diagnosing S3 (AUROC, 0.94 vs. 0.87; P=0.047). In addition, there was neither technical failure nor unreliable measurements in 2D-SWE and ATI examinations in this study, which could be a potential advantage of 2D-SWE and ATI for the evaluation of NAFLD. In contrast, there were three patients who had unreliable measurement results of TE and were subsequently excluded from the final analysis.

Since the introduction of CAP from TE in routine clinical practice, many studies have reported the diagnostic performance of CAP for the evaluation of hepatic steatosis during the past decade [10–14]. In a large-scale prospective study of 5,323 patients including all etiologies, the AUROC of ≥S1 (>10%) was reported as 0.79, that of ≥S2 was 0.84, and that of ≥S3 was 0.84 [17]. In a study conducted

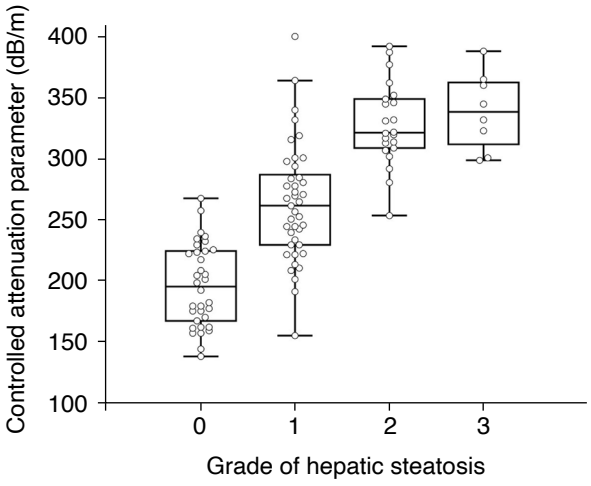

A

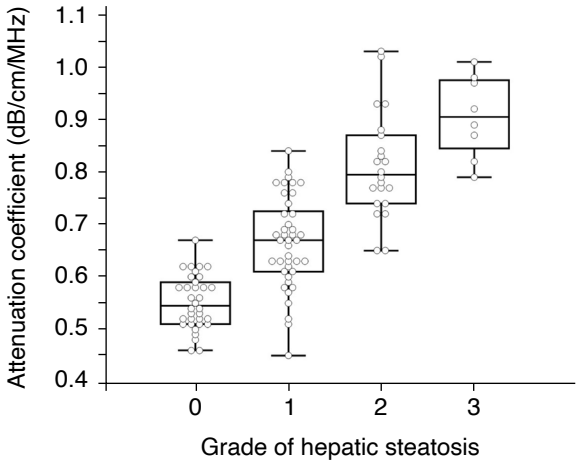

B

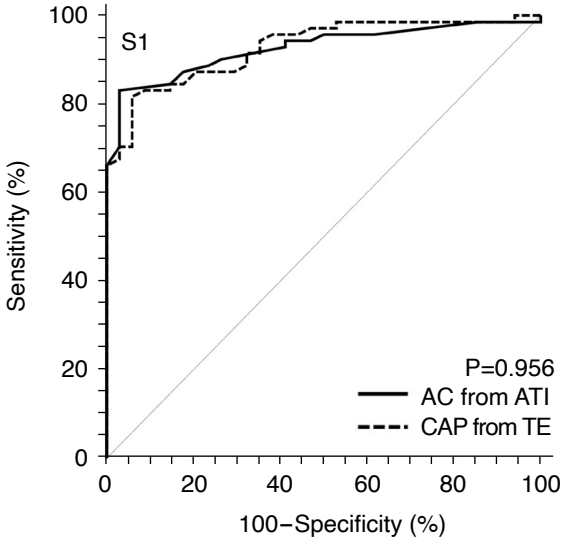

C

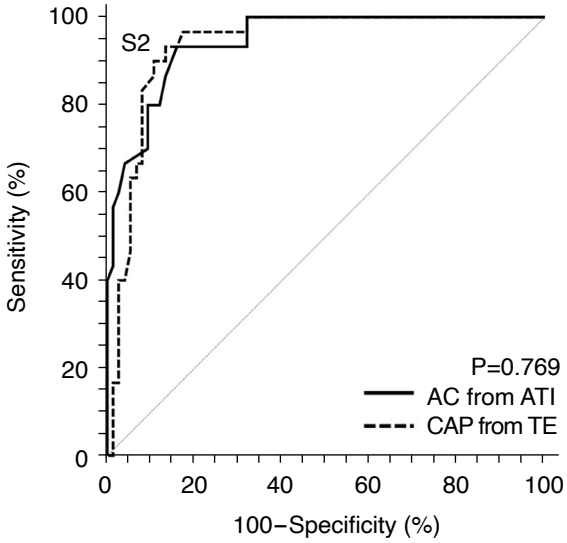

D

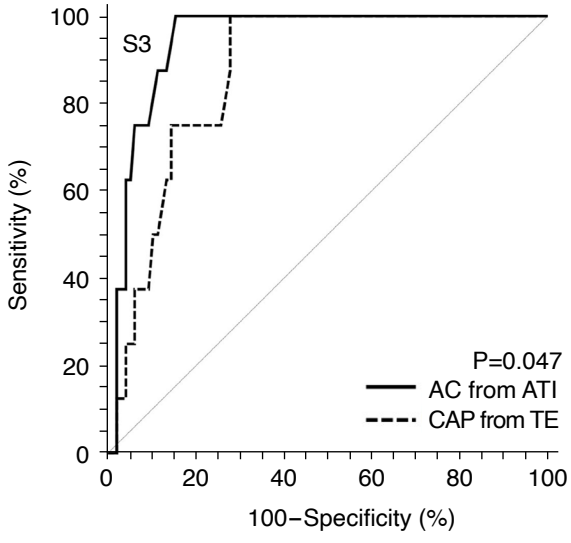

E

Fig. 2. Box-and-whisker plots showing (A) the controlled attenuation parameter (CAP) from transient elastography (TE), and (B) the attenuation coefficient (AC) from attenuation imaging (ATI) according to the grade of hepatic steatosis.
The box represents the interquartile range (25th–75th percentile), and the middle line represents the median value of CAP (A) and AC (B). Graphs show the area under the receiver operating characteristic curve (AUROC) of both CAP from TE and AC from ATI for diagnosing steatosis grade ≥S1 (C), ≥S2 (D), and ≥S3 (E). There was no significant difference between CAP and AC in detecting ≥S1 (0.93 vs. 0.93, P=0.956) and ≥S2 (0.94 vs. 0.94, P=0.769) (C, D). However, the AUROC of AC from ATI for detecting ≥S3 was significantly higher than that of CAP from TE (0.94 vs. 0.87, P=0.047) (E).

Table 3. Evaluation of liver fibrosis using liver stiffness values from 2D-SWE and TE

	≥F1	≥F2	≥F3	≥F4
Liver stiffness from 2D-SWE				
AUROC (95% CI)	0.89 (0.81–0.94)	0.90 (0.83–0.95)	0.90 (0.83–0.95)	0.88 (0.87–0.97)
Prevalence (n)	42	17	12	5
Cutoff (kPa)	6.0	7.1	7.7	8.8
Sensitivity	0.79 (33/42)	0.94 (16/17)	0.92 (11/12)	0.80 (4/5)
Specificity	0.84 (53/63)	0.86 (76/88)	0.84 (78/93)	0.85 (85/100)
PPV	0.77 (33/43)	0.57 (16/28)	0.42 (11/26)	0.21 (4/19)
NPV	0.85 (53/62)	0.99 (76/77)	0.99 (78/79)	0.99 (85/86)
Liver stiffness from TE				
AUROC (95% CI)	0.94 (0.88–0.98)	0.89 (0.81–0.94)	0.91 (0.84–0.96)	0.92 (0.85–0.96)
Prevalence (n)	42	17	12	5
Cutoff (kPa)	5.9	7.0	8.8	9.3
Sensitivity	0.88 (37/42)	0.71 (12/17)	0.83 (10/12)	0.80 (4/5)
Specificity	0.84 (53/63)	0.82 (72/88)	0.89 (83/93)	0.86 (86/100)
PPV	0.79 (37/47)	0.43 (12/28)	0.50 (10/20)	0.22 (4/18)
NPV	0.91 (53/58)	0.94 (72/77)	0.98 (83/85)	0.99 (86/87)

2D-SWE, two-dimensional shear wave elastography; TE, transient elastography; AUROC, area under the receiver operating characteristic curve; CI, confidence interval; PPV, positive predictive value; NPV, negative predictive value.

on NASH patients in the United Kingdom, the AUROC of ≥S1 was 0.87, that of ≥S2 was 0.77, and that of ≥S3 was 0.70 [19]. The AUROC of CAP in this study was 0.93 for ≥S1, 0.94 for ≥S2, and 0.87 for ≥S3, showing higher diagnostic performance than in previous studies. The difference in ethnic composition and distribution of the degree of hepatic steatosis might have affected the diagnostic performance of CAP in staging hepatic steatosis. In addition, the median BMI in this study was 24.2 kg/m^2, which is a lower value than those reported in previous studies. The lower BMI in this study also affected the results.

Since ATI is a new quantitative US technique, several studies using ATI to assess hepatic steatosis have been published [24–28]. In a study on NAFLD patients, the AUROC of steatosis diagnosis for ATI was 0.93 for ≥S1, 0.88 for ≥S2, and 0.83 for ≥S3 [20], similar to the results of our study. When we compared the diagnostic performance of ATI with that of CAP in detecting each grade of hepatic steatosis, there was no significant difference in the diagnosis of ≥S1 (AUROC of ATI: 0.93 vs. CAP: 0.93, P=0.956) and ≥S2 (AUROC of ATI: 0.94 vs. CAP: 0.94, P=0.769). However, the AUROC of ATI was significantly higher than that of CAP for the detection of ≥S3 (0.94 vs. 0.87, P=0.047). Because ATI is a B-mode-based quantitative US technique, the measurement ROI of ATI can be accurately placed onto the appropriate liver parenchyma, avoiding areas showing artifacts or large vessels under B-mode image guidance, which is an advantage of ATI over CAP, which involves blind measurements. Indeed, the measurement area of ATI would be larger than that of CAP. These theoretical advantages of ATI over TE might explain the results of this study, with ATI showing significantly better performance than CAP in the detection of ≥S3 steatosis.

In the diagnosis of fibrosis, TE is an extensively evaluated and validated diagnostic method, and many studies have been conducted on various chronic liver diseases [33–36]. Comparative studies between TE and 2D-SWE have also been carried out [37–40]. The pooled sensitivity and specificity of a meta-analysis for the diagnosis of fibrosis with TE in NAFLD showed a sensitivity of 79% and specificity of 75% for ≥F2, 85% and 95% for ≥F3, and 92% and 92% for ≥F4, respectively [36]. In a meta-analysis of 2D-SWE in NAFLD patients, the sensitivity and specificity were reported to be 93.8% and 52% for ≥F2, 93.1% and 80.9% for ≥F3, and 75.3% and 87.8% for ≥F4, respectively [23]. In a recent direct comparison study in NAFLD patients, the AUROCs of 2D-SWE and TE were 0.80 and 0.74 for ≥F2 and 0.91 and 0.87 for ≥F3, respectively, and there was no significant difference in AUROCs between the two elastography methods [38]. Similarly, in this study, there was no significant difference between 2D-SWE and TE in the comparison of AUROCs according to fibrosis stage. For the management of NAFLD patients, detection of ≥F2 fibrosis is clinically important since NAFLD with ≥F2 fibrosis is prone to progress to a more advanced stage of disease, including liver cirrhosis, leading to substantial morbidity and mortality [41]. Therefore, considering the results of previous

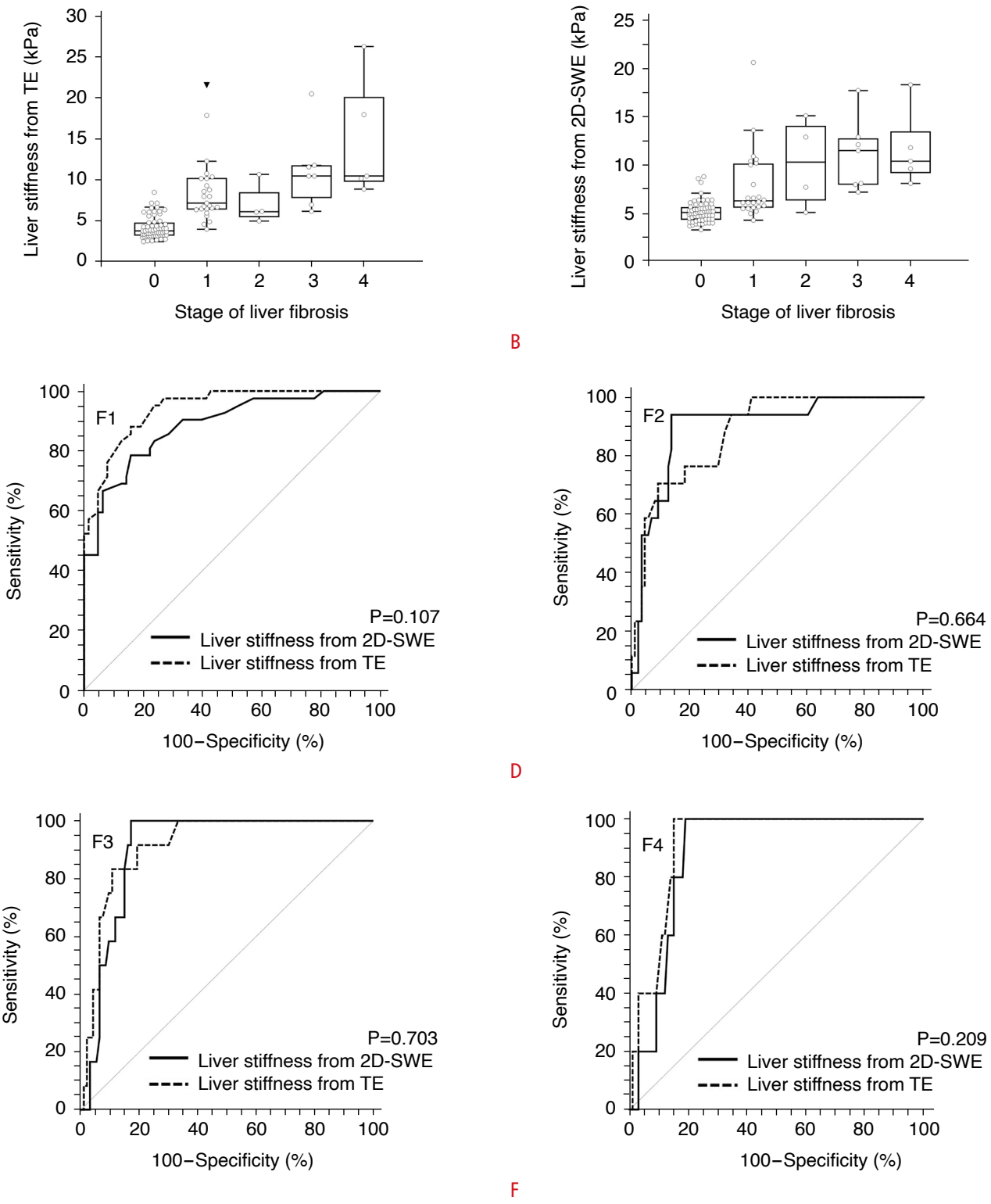

Fig. 3. Box-and-whisker plots showing liver stiffness (A) from transient elastography (TE) and (B) from two-dimensional shear wave elastography (2D-SWE) according to the stage of liver fibrosis. The box represents the interquartile range (25th–75th percentile), and the middle line represents the median value of liver stiffness from (A) TE and (B) 2D-SWE. Graphs show the area under the receiver operating characteristic curve of TE and 2D-SWE for diagnosing steatosis grade ≥F1 (C), ≥F2 (D), ≥F3 (E), and F4 (F). There was no significant difference between TE and 2D-SWE in all fibrosis stages; ≥F1 (0.94 vs. 0.89, P=0.107), ≥F2 (0.89 vs. 0.90, P=0.644), ≥F3 (0.91 vs. 0.90, P=0.703), and ≥F4 (0.88 vs. 0.92, P=0.209).

research and the present study, both TE and 2D-SWE would be good noninvasive methods to evaluate the liver fibrosis stage in NAFLD patients.

Since NAFLD patients require the assessment of both steatosis and fibrosis, a multiparametric approach using either TE with CAP or 2D-SWE with ATI is needed for a comprehensive evaluation [19,20]. In this study, ATI provided significantly better diagnostic performance for the detection of ≥S3 than CAP from TE. Regarding the evaluation of liver fibrosis, 2D-SWE showed diagnostic performance comparable to that of TE. In addition, 2D-SWE with ATI could provide B-mode US images of the liver simultaneously, enabling the evaluation of diffuse liver disease, hepatic masses, and the biliary system at the same time as quantitative measurements. Moreover, B-mode US examination of the liver is considered a primary or screening imaging test for patients suspected of having NAFLD based on abnormal laboratory tests. Given this background, the authors would cautiously suggest that 2D-SWE with ATI might be used as a primary imaging test for the evaluation of patients with NAFLD.

This study has several limitations. First, the retrospective selection of patients who underwent TE with CAP in a prospective study cohort may have introduced selection bias. However, the patient group of the population was selected prospectively, and among them, those who underwent TE with CAP were randomly selected. In addition, since the FibroScan method for each center is relatively standardized, both tests are not significantly different from those collected prospectively; thus, selection bias might have been minimized. Second, the distribution of fibrosis in this study showed high skewness, and most patients had either F0 or F1 stage fibrosis. With this skewed distribution, the exact assessment of diagnostic performance and cutoff values of TE and 2D-SWE in detecting ≥F3 and ≥F4 would be quite difficult, and the findings might be different from those of previous studies with different distributions of fibrosis stages. Third, in this study, only one US system from a single vendor (i.e., Aplio i800; Canon Medical Systems) was used for 2D-SWE and ATI examination. Therefore, further studies with different US systems from various vendors are warranted to generalize the results of this study. Fourth, the histopathology of liver specimens obtained from biopsy was evaluated at each center, and a central review was not performed. Therefore, there might have been a possibility of variability in the histopathologic examinations. Fifth, both M and XL probes were used for TE examinations in this study. Since the cutoff values might be different between the M and XL probes, this could be another limitation of this study.

In conclusion, 2D-SWE and TE showed comparable diagnostic performance in assessing liver fibrosis, and ATI provided significantly better performance in detecting ≥S3 than CAP. Therefore, a multiparametric approach using 2D-SWE with ATI might be helpful and could be used as a primary imaging test for the evaluation of NAFLD patients.

ORCID: Jung Wook Seo: https://orcid.org/0000-0002-5975-8698; Youe Ree Kim: https://orcid.org/0000-0001-5615-9721; Jong Keon Jang: https://orcid.org/0000-0002-2938-6635; So Yeon Kim: https://orcid.org/0000-0001-6853-8577; Young Youn Cho: https://orcid.org/0000-0002-9384-5357; Eun Sun Lee: https://orcid.org/0000-0003-0780-7985; Dong Ho Lee: https://orcid.org/0000-0001-8983-851X

Author Contributions

Conceptualization: Lee DH. Data acquisition: Seo JW, Kim YR, Jang JK, Kim SY, Cho YY, Lee ES, Lee DH. Data analysis or interpretation: Seo JW, Kim YR, Lee DH. Drafting of the manuscript: Seo JW, Kim YR. Critical revision of the manuscript: Jang JK, Kim SY, Cho YY, Lee ES, Lee DH. Approval of the final version of the manuscript: all authors.

Conflict of Interest

No potential conflict of interest relevant to this article was reported.

Supplementary Material

Supplementary Material 1. Patient enrollment status (https://doi.org/10.14366/usg.22212).

Supplementary Table 1. Determinant factors for each parameter derived from ultrasound examination (https://doi.org/10.14366/usg.22212).

Supplementary Table 2. Patient characteristics according to the grade of hepatic steatosis (https://doi.org/10.14366/usg.22212).

Supplementary Table 3. Evaluation of steatosis using attenuation coefficient and controlled attenuation parameters in patients with BMI less than 25 (n=58) (https://doi.org/10.14366/usg.22212).

Supplementary Table 4. Evaluation of steatosis using attenuation coefficient and controlled attenuation parameters in patients with BMI equal to or greater than 25 (n=47) (https://doi.org/10.14366/usg.22212).

Supplementary Table 5. Patient characteristics according to the stage of liver fibrosis (https://doi.org/10.14366/usg.22212).

Supplementary Table 6. Evaluation of liver fibrosis using liver stiffness value from 2D-SWE and TE in patients with BMI less than 25 (n=58) (https://doi.org/10.14366/usg.22212).

Supplementary Table 7. Evaluation of liver fibrosis using liver stiffness value from 2D-SWE and TE in patients with BMI equal to or

greater than 25 (n=47) (https://doi.org/10.14366/usg.22212).

References

1. Younossi ZM, Koenig AB, Abdelatif D, Fazel Y, Henry L, Wymer M. Global epidemiology of nonalcoholic fatty liver disease-Meta-analytic assessment of prevalence, incidence, and outcomes. Hepatology 2016;64:73-84.
2. Estes C, Razavi H, Loomba R, Younossi Z, Sanyal AJ. Modeling the epidemic of nonalcoholic fatty liver disease demonstrates an exponential increase in burden of disease. Hepatology 2018;67:123-133.
3. Estes C, Anstee QM, Arias-Loste MT, Bantel H, Bellentani S, Caballeria J, et al. Modeling NAFLD disease burden in China, France, Germany, Italy, Japan, Spain, United Kingdom, and United States for the period 2016-2030. J Hepatol 2018;69:896-904.
4. Ng CH, Huang DQ, Nguyen MH. Nonalcoholic fatty liver disease versus metabolic-associated fatty liver disease: prevalence, outcomes and implications of a change in name. Clin Mol Hepatol 2022;28:790-801.
5. Le MH, Yeo YH, Zou B, Barnet S, Henry L, Cheung R, et al. Forecasted 2040 global prevalence of nonalcoholic fatty liver disease using hierarchical bayesian approach. Clin Mol Hepatol 2022;28:841-850.
6. Sheka AC, Adeyi O, Thompson J, Hameed B, Crawford PA, Ikramuddin S. Nonalcoholic steatohepatitis: a review. JAMA 2020;323:1175-1183.
7. Kawaguchi T, Tsutsumi T, Nakano D, Eslam M, George J, Torimura T. MAFLD enhances clinical practice for liver disease in the Asia-Pacific region. Clin Mol Hepatol 2022;28:150-163.
8. Farrell GC, Larter CZ. Nonalcoholic fatty liver disease: from steatosis to cirrhosis. Hepatology 2006;43(2 Suppl 1):S99-S112.
9. Soon G, Wee A. Updates in the quantitative assessment of liver fibrosis for nonalcoholic fatty liver disease: histological perspective. Clin Mol Hepatol 2021;27:44-57.
10. Kang SH, Lee HW, Yoo JJ, Cho Y, Kim SU, Lee TH, et al. KASL clinical practice guidelines: Management of nonalcoholic fatty liver disease. Clin Mol Hepatol 2021;27:363-401.
11. Noureddin M, Vipani A, Bresee C, Todo T, Kim IK, Alkhouri N, et al. NASH leading cause of liver transplant in women: updated analysis of indications for liver transplant and ethnic and gender variances. Am J Gastroenterol 2018;113:1649-1659.
12. Rockey DC, Caldwell SH, Goodman ZD, Nelson RC, Smith AD; American Association for the Study of Liver Diseases. Liver biopsy. Hepatology 2009;49:1017-1044.
13. Schwenzer NF, Springer F, Schraml C, Stefan N, Machann J, Schick F. Non-invasive assessment and quantification of liver steatosis by ultrasound, computed tomography and magnetic resonance. J Hepatol 2009;51:433-445.
14. Ozturk A, Grajo JR, Gee MS, Benjamin A, Zubajlo RE, Thomenius KE, et al. Quantitative hepatic fat quantification in non-alcoholic fatty liver disease using ultrasound-based techniques: a review of literature and their diagnostic performance. Ultrasound Med Biol 2018;44:2461-2475.
15. Sasso M, Beaugrand M, de Ledinghen V, Douvin C, Marcellin P, Poupon R, et al. Controlled attenuation parameter (CAP): a novel VCTE guided ultrasonic attenuation measurement for the evaluation of hepatic steatosis: preliminary study and validation in a cohort of patients with chronic liver disease from various causes. Ultrasound Med Biol 2010;36:1825-1835.
16. Hong YM, Yoon KT, Cho M, Chu CW, Rhu JH, Yang KH, et al. Clinical usefulness of controlled attenuation parameter to screen hepatic steatosis for potential donor of living donor liver transplant. Eur J Gastroenterol Hepatol 2017;29:805-810.
17. de Ledinghen V, Vergniol J, Capdepont M, Chermak F, Hiriart JB, Cassinotto C, et al. Controlled attenuation parameter (CAP) for the diagnosis of steatosis: a prospective study of 5323 examinations. J Hepatol 2014;60:1026-1031.
18. Karlas T, Petroff D, Sasso M, Fan JG, Mi YQ, de Ledinghen V, et al. Individual patient data meta-analysis of controlled attenuation parameter (CAP) technology for assessing steatosis. J Hepatol 2017;66:1022-1030.
19. Eddowes PJ, Sasso M, Allison M, Tsochatzis E, Anstee QM, Sheridan D, et al. Accuracy of FibroScan controlled attenuation parameter and liver stiffness measurement in assessing steatosis and fibrosis in patients with nonalcoholic fatty liver disease. Gastroenterology 2019;156:1717-1730.
20. Lee DH, Cho EJ, Bae JS, Lee JY, Yu SJ, Kim H, et al. Accuracy of two-dimensional shear wave elastography and attenuation imaging for evaluation of patients with nonalcoholic steatohepatitis. Clin Gastroenterol Hepatol 2021;19:797-805.
21. Sugimoto K, Moriyasu F, Oshiro H, Takeuchi H, Abe M, Yoshimasu Y, et al. The role of multiparametric US of the liver for the evaluation of nonalcoholic steatohepatitis. Radiology 2020;296:532-540.
22. Sugimoto K, Lee DH, Lee JY, Yu SJ, Moriyasu F, Sakamaki K, et al. Multiparametric US for identifying patients with high-risk NASH: a derivation and validation study. Radiology 2021;301:625-634.
23. Herrmann E, de Ledinghen V, Cassinotto C, Chu WC, Leung VY, Ferraioli G, et al. Assessment of biopsy-proven liver fibrosis by two-dimensional shear wave elastography: an individual patient data-based meta-analysis. Hepatology 2018;67:260-272.
24. Tamaki N, Koizumi Y, Hirooka M, Yada N, Takada H, Nakashima O, et al. Novel quantitative assessment system of liver steatosis using a newly developed attenuation measurement method. Hepatol Res 2018;48:821-828.
25. Han A, Andre MP, Deiranieh L, Housman E, Erdman JW, Jr., Loomba R, et al. Repeatability and reproducibility of the ultrasonic attenuation coefficient and backscatter coefficient measured

in the right lobe of the liver in adults with known or suspected nonalcoholic fatty liver disease. J Ultrasound Med 2018;37:1913-1927.
26. Bae JS, Lee DH, Lee JY, Kim H, Yu SJ, Lee JH, et al. Assessment of hepatic steatosis by using attenuation imaging: a quantitative, easy-to-perform ultrasound technique. Eur Radiol 2019;29:6499-6507.
27. Jeon SK, Lee JM, Joo I, Yoon JH, Lee DH, Lee JY, et al. Prospective evaluation of hepatic steatosis using ultrasound attenuation imaging in patients with chronic liver disease with magnetic resonance imaging proton density fat fraction as the reference standard. Ultrasound Med Biol 2019;45:1407-1416.
28. Tada T, Iijima H, Kobayashi N, Yoshida M, Nishimura T, Kumada T, et al. Usefulness of attenuation imaging with an ultrasound scanner for the evaluation of hepatic steatosis. Ultrasound Med Biol 2019;45:2679-2687.
29. Jang JK, Lee ES, Seo JW, Kim YR, Kim SY, Cho YY, et al. Two-dimensional shear-wave elastography and US attenuation imaging for nonalcoholic steatohepatitis diagnosis: a cross-sectional, multicenter study. Radiology 2022;305:118-126.
30. Ferraioli G, Filice C, Castera L, Choi BI, Sporea I, Wilson SR, et al. WFUMB guidelines and recommendations for clinical use of ultrasound elastography: Part 3: liver. Ultrasound Med Biol 2015;41:1161-1179.
31. Dietrich CF, Bamber J, Berzigotti A, Bota S, Cantisani V, Castera L, et al. EFSUMB guidelines and recommendations on the clinical use of liver ultrasound elastography, update 2017 (long version). Ultraschall Med 2017;38:e16-e47.
32. Kleiner DE, Brunt EM, Van Natta M, Behling C, Contos MJ, Cummings OW, et al. Design and validation of a histological scoring system for nonalcoholic fatty liver disease. Hepatology 2005;41:1313-1321.
33. Friedrich-Rust M, Ong MF, Martens S, Sarrazin C, Bojunga J, Zeuzem S, et al. Performance of transient elastography for the staging of liver fibrosis: a meta-analysis. Gastroenterology 2008;134:960-974.
34. Tsochatzis EA, Gurusamy KS, Ntaoula S, Cholongitas E, Davidson BR, Burroughs AK. Elastography for the diagnosis of severity of fibrosis in chronic liver disease: a meta-analysis of diagnostic accuracy. J Hepatol 2011;54:650-659.
35. Myers RP, Pomier-Layrargues G, Kirsch R, Pollett A, Duarte-Rojo A, Wong D, et al. Feasibility and diagnostic performance of the FibroScan XL probe for liver stiffness measurement in overweight and obese patients. Hepatology 2012;55:199-208.
36. Kwok R, Tse YK, Wong GL, Ha Y, Lee AU, Ngu MC, et al. Systematic review with meta-analysis: non-invasive assessment of non-alcoholic fatty liver disease: the role of transient elastography and plasma cytokeratin-18 fragments. Aliment Pharmacol Ther 2014;39:254-269.
37. Lee DH, Lee ES, Bae JS, Lee JY, Han JK, Yi NJ, et al. 2D shear wave elastography is better than transient elastography in predicting post-hepatectomy complication after resection. Eur Radiol 2021;31:5802-5811.
38. Furlan A, Tublin ME, Yu L, Chopra KB, Lippello A, Behari J. Comparison of 2D shear wave elastography, transient elastography, and MR elastography for the diagnosis of fibrosis in patients with nonalcoholic fatty liver disease. AJR Am J Roentgenol 2020;214:W20-W26.
39. Thiele M, Detlefsen S, Sevelsted Moller L, Madsen BS, Fuglsang Hansen J, Fialla AD, et al. Transient and 2-dimensional shear-wave elastography provide comparable assessment of alcoholic liver fibrosis and cirrhosis. Gastroenterology 2016;150:123-133.
40. Zeng J, Zheng J, Huang Z, Chen S, Liu J, Wu T, et al. Comparison of 2-D shear wave elastography and transient elastography for assessing liver fibrosis in chronic hepatitis B. Ultrasound Med Biol 2017;43:1563-1570.
41. Angulo P, Kleiner DE, Dam-Larsen S, Adams LA, Bjornsson ES, Charatcharoenwitthaya P, et al. Liver fibrosis, but no other histologic features, is associated with long-term outcomes of patients with nonalcoholic fatty liver disease. Gastroenterology 2015;149:389-397.

Supplementary Material 1. Patient enrollment status.

Institutional review board of each participating center approved retrospective analysis of previous nonalcoholic fatty liver disease (NAFLD) cohort (IRB number: H-2210-139-1373 for Seoul National University Hospital, WKUH 2022-11-012 for Wonkwang University Hospital, ISPAIK 2022-10-006 for Ilsan Paik Hospital, 2210-005-19439 for Chung-Ang University Hospital, 2022-1584 for Asan Medical Center). Among the 132 participants of previous cohort, 105 participants met the inclusion criteria for this study. Among them, 58 participants were potential living liver donors who underwent liver biopsy to evaluate NAFLD for decision regarding the liver donor eligibility. All of potential liver donors were enrolled from Asan Medical Center. Remaining 47 participants underwent liver biopsy under the clinical suspicion of NAFLD: 14 participants from Seoul national university hospital; 13 participants from Asan medical center; 11 participants from Chung-Ang University Hospital; six participants from Ilsan Paik Hospital; and three participants from Wonkwang University Hospital.

Supplementary Table 1. Determinant factors for each parameter derived from ultrasound examination

US parameter	Characteristic	Univariate analysis			Multivariate analysis		
		Coefficient	95% CI	P-value	Coefficient	95% CI	P-value
Attenuation coefficient (dB/cm/MHz) from ATI	Fibrosis	0.039	0.016 to 0.061	0.001	−0.016	−0.053 to 0.001	0.065
	Lobular inflammation activity	0.080	0.056 to 0.103	<0.001	0.015	−0.018 to 0.047	0.373
	Hepatocyte ballooning	0.092	0.059 to 0.125	<0.001	0.025	−0.018 to 0.068	0.246
	Steatosis	0.122	0.105 to 0.139	<0.001	0.121	0.097 to 0.146	<0.001
	Age (year)	0.001	−0.001 to 0.003	0.170			
	Male sex	−0.027	−0.080 to 0.026	0.320			
	Body mass index (kg/m^2)	0.014	0.007 to 0.020	<0.001	0.003	−0.002 to 0.007	0.267
	ALT (IU/L)	0.001	0.001 to 0.001	<0.001	0.000	−0.001 to 0.001	0.483
	AST (IU/L)	0.002	0.001 to 0.002	<0.001	−0.001	−0.002 to 0.001	0.172
Liver stiffness (kPa) from 2D-SWE	Fibrosis	1.863	1.439 to 2.287	<0.001	0.993	0.242 to 1.744	0.010
	Lobular inflammation activity	1.741	1.168 to 2.315	<0.001	−0.341	−1.292 to 0.610	0.478
	Hepatocyte ballooning	2.899	2.211 to 3.588	<0.001	1.101	−0.146 to 2.349	0.083
	Steatosis	1.724	1.111 to 2.338	<0.001	0.708	−0.016 to 1.432	0.055
	Age (year)	0.095	0.059 to 0.131	<0.001	0.015	−0.024 to 0.053	0.453
	Male sex	0.494	−0.770 to 1.757	0.440			
	Body mass index (kg/m^2)	0.339	0.191 to 0.486	<0.001	0.183	0.051 to 0.314	0.007
	ALT (IU/L)	0.012	0.003 to 0.022	0.012	−0.014	−0.030 to 0.002	0.079
	AST (IU/L)	0.031	0.014 to 0.048	<0.001	0.016	−0.013 to 0.044	0.279
Controlled attenuation parameter (dB/m) from TE	Fibrosis	26.57	16.69 to 36.45	<0.001	−4.657	−16.47 to 7.16	0.436
	Lobular inflammation activity	37.53	26.44 to 48.62	<0.001	−6.075	−24.03 to 8.875	0.422
	Hepatocyte ballooning	49.75	34.84 to 64.65	<0.001	6.940	−12.68 to 26.56	0.484
	Steatosis	56.60	48.18 to 65.01	0.002	53.53	42.15 to 64.91	<0.001
	Age (year)	1.376	0.609 to 2.144	0.001	0.740	0.945 to 5.078	0.016
	Male sex	−3.610	−28.87 to 21.64	0.777			
	Body mass index (kg/m^2)	7.758	4.925 to 10.59	<0.001	3.012	0.945 to 5.078	0.005
	ALT (IU/L)	0.475	0.305 to 0.645	<0.001	0.116	−0.136 to 0.367	0.364
	AST (IU/L)	0.825	0.512 to 1.138	<0.001	−0.271	−0.722 to 0.181	0.237
Liver stiffness (kPa) from 2TE	Fibrosis	2.513	1.981 to 3.045	<0.001	1.515	0.579 to 2.451	0.002
	Lobular inflammation activity	2.476	1.760 to 3.192	<0.001	−1.067	−2.251 to 0.117	0.077
	Hepatocyte ballooning	4.086	3.251 to 4.920	<0.001	2.066	0.512 to 3.620	0.010
	Steatosis	2.366	1.585 to 3.146	<0.001	0.457	−0.445 to 1.358	0.317
	Age (year)	0.112	0.064 to 0.160	<0.001	0.007	−0.041 to 0.055	0.767
	Male sex	−0.090	−1.733 to 1.552	0.913			
	Body mass index (kg/m^2)	0.422	0.229 to 0.615	<0.001	0.130	−0.034 to 0.294	0.118
	ALT (IU/L)	0.027	0.016 to 0.039	<0.001	0.004	−0.016 to 0.024	0.667
	AST (IU/L)	0.056	0.036 to 0.076	<0.001	0.013	−0.022 to 0.049	0.458

CI, confidence interval; ATI, attenuation imaging; ALT, alanine aminotransferase; IU, international unit; AST, aspartate aminotransferase; SWE, shear wave elastography; TE, transient elastography.

Supplementary Table 2. Patient characteristics according to the grade of hepatic steatosis

	S0 (n=34)	S1 (n=41)	S2 (n=22)	S3 (n=8)
Age (year)	30.5 (27.0–37.0)	38.0 (26.8–54.5)	48.0 (43.0–63.0)	34.0 (22.0–47.0)
Sex (male:female)	15:19	23:18	11:11	4:4
Body mass index (kg/m^2)	21.8 (20.7–25.1)	25.2 (23.1–27.2)	26.4 (24.0–30.7)	23.6 (22.7–27.0)
Hypertension	4 (11.8)	13 (31.7)	13 (59.1)	1 (12.5)
Diabetes mellitus	0	5 (12.2)	11 (50.0)	4 (50.0)
ALT (IU/L)	10.5 (8.0–18.0)	22.0 (14.8–37.0)	58.5 (40.0–88.0)	168.0 (30.0–246.5)
AST (IU/L)	17.5 (15.0–21.0)	21.0 (17.0–33.8)	43.5 (25.0–60.0)	98.0 (63.5–139.5)
Albumin (mg/dL)	4.2 (4.1–4.4)	4.4 (4.1–4.5)	4.2 (4.0–4.5)	4.2 (3.0–5.0)
Total bilirubin (mg/dL)	0.6 (0.4–0.8)	0.7 (0.5–1.0)	0.6 (0.4–0.6)	1.0 (0.3–1.4)
PT-INR	1.03 (0.95–1.09)	1.01 (0.98–1.07)	1.00 (0.97–1.01)	1.07 (1.01–1.16)

Values are presented as median (IQR) or number (%).
ALT, alanine aminotransferase; AST, aspartate aminotransferase; PT-INR, prothrombin time international normalized ratio; IQR, interquartile range.

Supplementary Table 3. Evaluation of steatosis using attenuation coefficient and controlled attenuation parameters in patients with BMI less than 25 (n=58)

	≥S1 (≥5% steatosis)	≥S2 (≥34% steatosis)	≥S3 (≥67% steatosis)
Attenuation coefficient from ATI			
AUROC (95% CI)	0.93 (0.83–0.98)	0.99 (0.92–1.00)	0.99 (0.91–1.00)
Prevalence (n)	33	13	5
Cutoff (dB/cm/MHz)	0.62	0.72	0.83
Sensitivity	0.82 (27/33)	1.00 (13/13)	1.00 (5/5)
Specificity	0.96 (24/25)	0.93 (42/45)	0.96 (51/53)
PPV	0.96 (27/28)	0.81 (13/16)	0.71 (5/7)
NPV	0.80 (24/30)	1.00 (42/42)	1.00 (51/51)
Controlled attenuation parameter from TE			
AUROC (95% CI)	0.93 (0.83–0.98)	0.99 (0.92–1.00)	0.94 (0.84–0.98)
Prevalence (n)	33	13	5
Cutoff (dB/m)	209	298	298
Sensitivity	0.94 (31/33)	1.00 (13/13)	1.00 (5/5)
Specificity	0.76 (19/25)	0.96 (43/45)	0.81 (43/53)
PPV	0.84 (31/37)	0.87 (13/15)	0.33 (5/15)
NPV	0.90 (19/21)	1.00 (43/43)	1.00 (43/43)

BMI, body mass index; ATI, attenuation imaging; AUROC, area under the receiver operating characteristic curve; CI, confidence interval; PPV, positive predictive value; NPV, negative predictive value; TE, transient elastography.

Supplementary Table 4. Evaluation of steatosis using attenuation coefficient and controlled attenuation parameters in patients with BMI equal to or greater than 25 (n=47)

	≥S1 (≥5% steatosis)	≥S2 (≥34% steatosis)	≥S3 (≥67% steatosis)
Attenuation coefficient from ATI			
AUROC (95% CI)	0.92 (0.81–0.98)	0.88 (0.75–0.96)	0.87 (0.74–0.95)
Prevalence (n)	38	17	3
Cutoff (dB/cm/MHz)	0.62	0.69	0.78
Sensitivity	0.84 (32/38)	0.88 (15/17)	1.00 (3/3)
Specificity	1.00 (9/9)	0.73 (22/30)	0.80 (35/44)
PPV	1.00 (32/32)	0.65 (15/23)	0.25 (3/12)
NPV	0.60 (9/15)	0.92 (22/24)	1.00 (35/35)
Controlled attenuation parameter from TE			
AUROC (95% CI)	0.94 (0.82–0.99)	0.86 (0.73–0.94)	0.80 (0.66–0.90)
Prevalence (n)	38	17	3
Cutoff (dB/m)	240	285	294
Sensitivity	0.92 (35/38)	0.88 (15/17)	1.00 (3/3)
Specificity	1.00 (9/9)	0.77 (23/30)	0.61 (27/44)
PPV	1.00 (35/35)	0.68 (15/22)	0.15 (3/20)
NPV	0.75 (9/12)	0.92 (23/25)	1.00 (27/27)

BMI, body mass index; ATI, attenuation imaging; AUROC, area under the receiver operating characteristic curve; CI, confidence interval; PPV, positive predictive value; NPV, negative predictive value; TE, transient elastography.

Supplementary Table 5. Patient characteristics according to the stage of liver fibrosis

	F0 (n=63)	F1 (n=25)	F2 (n=5)	F3 (n=7)	F4 (n=5)
Age (year)	31.0 (25.0–38.0)	44.0 (27.8–51.5)	62.0 (47.5–66.5)	63.0 (53.3–66.8)	63.0 (57.8–69.8)
Sex (male:female)	32:31	12:13	2:3	5:2	2:3
Body mass index (kg/m^2)	23.3 (20.9–26.2)	25.4 (23.6–31.2)	25.2 (22.2–29.4)	26.9 (24.8–28.9)	27.3 (25.1–28.2)
Hypertension	14	6	2	4	5
Diabetes mellitus	0	7	4	5	4
ALT (IU/L)	14.0 (9.0–19.8)	75.0 (42.8–124.0)	32.0 (19.0–64.0)	73.0 (47.0–112.0)	28.0 (26.0–79.8)
AST (IU/L)	18.0 (15.0–21.8)	54.0 (26.0–96.0)	50.0 (26.3–85.0)	60.0 (52.3–65.5)	42.0 (27.3–56.5)
Albumin (mg/dL)	4.3 (4.1–4.5)	4.4 (4.0–4.6)	3.6 (2.7–3.7)	4.3 (4.1–4.5)	4.0 (3.6–4.2)
Total bilirubin (mg/dL)	0.6 (0.5–0.9)	0.6 (0.4–1.1)	0.8 (0.4–1.4)	0.6 (0.4–0.6)	0.5 (0.4–0.7)
PT-INR	1.02 (0.97–1.06)	1.01 (0.99–1.08)	1.12 (1.01–1.30)	0.98 (0.96–1.00)	1.01 (0.98–1.17)

Values are presented as median (IQR) or number (%).

IQR, interquartile range; ALT, alanine aminotransferase; AST, aspartate aminotransferase; PT-INR, prothrombin time international normalized ratio.

Supplementary Table 6. Evaluation of liver fibrosis using liver stiffness value from 2D-SWE and TE in patients with BMI less than 25 (n=58)

	≥F1	≥F2	≥F3	≥F4
Liver stiffness from 2D-SWE				
AUROC (95% CI)	0.89 (0.78–0.96)	0.97 (0.89–1.00)	0.91 (0.81–0.97)	NA
Prevalence (n)	16	5	3	1
Cutoff (kPa)	6.0	6.4	8.0	NA
Sensitivity	0.75 (12/16)	1.00 (5/5)	0.67 (2/3)	NA
Specificity	0.93 (39/42)	0.89 (47/53)	0.87 (48/55)	NA
PPV	0.80 (12/15)	0.45 (5/11)	0.22 (2/9)	NA
NPV	0.91 (39/43)	1.00 (47/47)	0.98 (48/49)	NA
Liver stiffness from TE				
AUROC (95% CI)	0.92 (0.81–0.97)	0.94 (0.84–0.98)	0.97 (0.89–1.00)	NA
Prevalence (n)	16	5	3	1
Cutoff (kPa)	4.8	6.1	9.3	NA
Sensitivity	0.94 (15/16)	0.80 (4/5)	1.00 (3/3)	NA
Specificity	0.79 (33/42)	0.74 (39/53)	0.96 (51/53)	NA
PPV	0.63 (15/24)	0.22 (4/18)	0.60 (3/5)	NA
NPV	0.97 (33/34)	0.98 (39/40)	1.00 (51/51)	NA

2D-SWE, two-dimensional shear wave elastography; TE, transient elastography; BMI, body mass index; AUROC, area under the receiver operating characteristic curve; CI, confidence interval; PPV, positive predictive value; NPV, negative predictive value; NA, not available.

Supplementary Table 7. Evaluation of liver fibrosis using liver stiffness value from 2D-SWE and TE in patients with BMI equal to or greater than 25 (n=47)

	≥F1	≥F2	≥F3	≥F4
Liver stiffness from 2D-SWE				
AUROC (95% CI)	0.85 (0.72–0.94)	0.83 (0.69–0.92)	0.87 (0.74–0.95)	0.84 (0.70–0.93)
Prevalence (n)	26	12	9	4
Cutoff (kPa)	6.4	7.1	8.1	10.4
Sensitivity	0.73 (19/26)	0.92 (11/12)	0.67 (6/9)	0.75 (3/4)
Specificity	0.90 (19/21)	0.83(29/35)	0.82 (31/38)	0.79 (34/43)
PPV	0.90 (19/21)	0.65 (11/17)	0.46 (6/13)	0.25 (3/12)
NPV	0.73 (19/26)	0.97 (29/30)	0.91 (31/34)	0.97 (34/35)
Liver stiffness from TE				
AUROC (95% CI)	0.96 (0.86–1.00)	0.82 (0.68–0.92)	0.87 (0.74–0.95)	0.89 (0.77–0.96)
Prevalence (n)	26	12	9	4
Cutoff (kPa)	5.9	6.8	8.8	10.4
Sensitivity	0.88 (23/26)	0.75 (9/12)	0.78 (7/9)	0.75 (3/4)
Specificity	0.90 (19/21)	0.74 (26/35)	0.82 (31/38)	0.84 (36/43)
PPV	0.92 (23/25)	0.50 (9/18)	0.50 (7/14)	0.30 (3/10)
NPV	0.86 (19/22)	0.90 (26/29)	0.94 (31/33)	0.97 (36/37)

2D-SWE, two-dimensional shear wave elastography; TE, transient elastography; BMI, body mass index; AUROC, area under the receiver operating characteristic curve; CI, confidence interval; PPV, positive predictive value; NPV, negative predictive value.